Optimization of Deposition Uniformity for Large-Aperture NIF Substrates in a Planetary Rotation System

Introduction

Large substrates for precision optical applications require the accurate, uniform deposition of multilayer thin-film coatings. Typically, this results in the use of electron-beam evaporation in a "box-coater" configuration, utilizing either simple or planetary rotation of the substrates. Simple rotation of the substrate minimizes the size of the necessary coating chamber but generally results in films with nonuniformity of 2% or greater,[1] an unacceptable level for the precise requirements of the National Ignition Facility (NIF). Typical planetary rotation systems, containing four to five individual substrate holders, or planets, tend to produce relatively uniform coatings but would necessarily be quite large in order to process optics of a significant size. To process large optics for the NIF, a counter-rotating planetary geometry was developed and implemented in a 72-in. electron-beam deposition system.[2] Although this rotation system utilizes planetary motion to reduce the effect of deposition fluctuations, the large optic sizes relative to the overall chamber size and geometry result in coatings with a significant degree of nonuniformity if regions of the vapor plume are not masked.

To achieve the goal of producing optical coatings with nonuniformities of approximately 0.5% (peak-to-valley) over apertures of 0.85 m, a careful model needs to be constructed to account for deposition sources, planetary configuration, planetary gearing, and uniformity masking. The model assumes that the chamber and source conditions are quite stable throughout the length of the deposition, requiring a highly deterministic process. The process uses metallic hafnia for high-index layers and granular silica for low-index layers to produce coatings with exceptional resistance to high-peak-power laser irradiation.[3,4] The use of hafnium metal as an evaporant is ideal due to the smooth melt surface, the low occurrence of nodular defects in the growing film, and the stable chemical composition of the melt throughout the length of the deposition. Silica deposition tends to pose some difficulties, but its use is necessitated by the lack of a suitable substitute for precision laser coatings; electron-beam sweep parameters, deposition rate, and oxygen backfill pressure were optimized to minimize process variability.

Background

The uniform deposition of a thin film applied over a surface from a point or surface source can essentially be characterized as an illumination problem, with the appropriate type of source characterization. The theoretical equations governing the amount of material deposited on a given area have been well established;[5–9] therefore the results specific to a given chamber configuration simply become a summation of incremental thickness contributions as the planet position is indexed through the chamber. Since the system under study uses electron-beam sources, the source may be considered to be of the directed surface source type, with

$$t = \left(\frac{m}{\pi\mu}\right)\left(\frac{\cos\phi\cos\theta}{r^2}\right), \tag{1}$$

where t is the thickness of the film deposited, m is the total mass of the material emitted from the source, μ is the density of the film being deposited, ϕ is the angle normal to the surface of the source, θ is the angle normal to the substrate surface, and r is the distance from the source to the point on the substrate under evaluation (see Fig. 94.1). However, since the primary concern is uniformity of the deposited film, once the summation is performed for all of the incremental planar positions, the relative thicknesses will be normalized over the surface of the substrates being coated. When the thicknesses are normalized, the constants in Eq. (1) will cancel, resulting in the simplified expression

$$t = \frac{\cos\phi\cos\theta}{r^2}. \tag{2}$$

The geometry may be further simplified to reflect that the source surface is parallel to that of the surface being coated; such a condition would not be appropriate for a tilted-planet

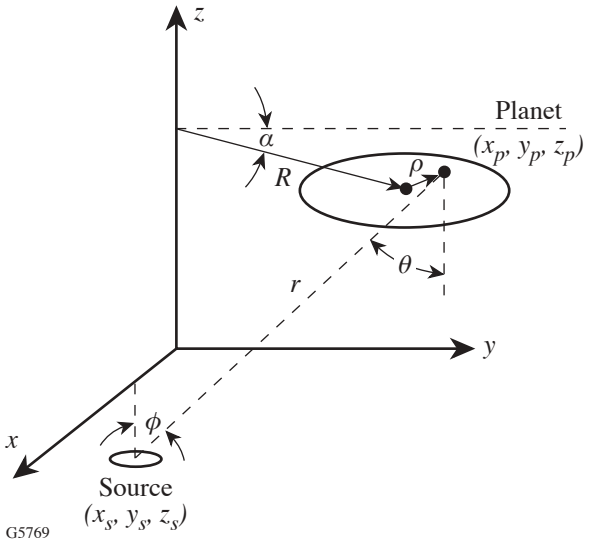

Figure 94.1
Basic planetary configuration as substrate undergoes rotations/revolution.

rotation but is applicable for a standard planetary with all surfaces being coated rotating in a plane. In this case,

$$t = \frac{\cos^2\theta}{r^2}. \tag{3}$$

This expression is appropriate for an ideal directed-surface source, but measurements of film uniformity indicate factors such as the form of the material being evaporated, the electron-beam sweep parameters, and the proximity of the source to the walls of the coating chamber possibly affecting the accuracy of this formula. In practice, the formula may be modified to[9]

$$t = \frac{\cos^n\theta}{r^2}, \tag{4}$$

where n is now a variable allowing the theoretical thickness distribution to be fit to that of the measured distribution. Converting this to coordinate geometry,

$$r = \sqrt{\left(x_p - x_s\right)^2 + \left(y_p - y_s\right)^2 + \left(z_p - z_s\right)^2} \tag{5}$$

and

$$\cos\theta = \frac{z_p - z_s}{\sqrt{\left(x_p - x_s\right)^2 + \left(y_p - y_s\right)^2 + \left(z_p - z_s\right)^2}}, \tag{6}$$

where the subscript "p" denotes the point on the planet and "s" denotes the source. Substitution and simplification then yield

$$t = \left\{\frac{\left(z_p - z_s\right)^n}{\left[\left(x_p - x_s\right)^2 + \left(y_p - y_s\right)^2 + \left(z_p - z_s\right)^2\right]^{\frac{n+2}{2}}}\right\}. \tag{7}$$

The coordinates of the source(s), as well as the height of the substrates, will be measured quantities to be inserted into the deposition model. The x and y coordinates of a given point being tracked in the planetary must be calculated, based on Fig. 94.1. Given the relation as shown, the primary factor in determining the motion of a point on the planet will be the relative angular rotation of the planet to that of the revolution of the system, which is simply a function of the relative gear sizes for the solar and planet gears. This will be explored in greater detail later, but the motion of a point on the planet undergoing planetary rotation will trace out the path described by

$$x(\alpha) = R\cos\alpha + \rho\cos\left(\frac{\alpha N_s}{N_p}\right) \tag{8}$$

and

$$y(\alpha) = R\sin\alpha + \rho\sin\left(\frac{\alpha N_s}{N_p}\right), \tag{9}$$

where R is the radius of the planet orbit, ρ is the radial position of the point on the planet, α is the angular position of the planet in its orbit, and N_s and N_p are the number of teeth on the solar and planet gears, respectively. Since the planets are rotating in-plane, z_p will remain constant and the thickness contribution at any point in the planetary motion can now be calculated as a function of only α. A summation of the individual contributions throughout a number of revolutions, where α is incremented from 0 to 2π, and for a range of ρ from the center to the edge of the planet, will provide an overall uniformity distribution over the surface of the planet.

Coating efficiency is also of interest when configuring the planetary rotation system since configurations can be conceived that provide nearly ideal uniformity, but due to signifi-

cant offsets of the source from the center of rotation or excessive distances between the substrate and the source, the percentage of vaporized material condensing on the substrates is negligible. Therefore, since the desired result is to achieve a high degree of film uniformity while maximizing source material utilization, it is necessary to calculate the percentage of evaporated material being deposited on the substrate.

The motion of a typical planetary rotation describes an annulus in the plane of rotation since the planets orbit at a constant radius without crossing the center of the chamber. Since the planets in the counter-rotating configuration cross the center of the chamber, a disk replaces the annulus and the efficiency becomes the percentage of deposited material within this disk. The efficiency with which evaporated source material is used is equal to the integral of Eq. (4) over the area defined by the disk, divided by the integral of Eq. (4) over the hemisphere above the source, i.e., the range of θ from 0 to $\pi/2$. The integration over a hemisphere is straightforward, resulting in a normalization value of π:

$$\text{Efficiency} = \frac{1}{\pi} \int_{\substack{\text{over}\\ \text{disc}}} \int \frac{\cos^{n+1}\theta}{r^2} d\gamma\, d\theta. \qquad (10)$$

The integration of an off-axis source, as shown in Fig. 94.2, is transformed to that of an on-axis source in order to easily and accurately express the limits of integration. Performing the transformation, the efficiency of the source is found to be

$$\text{Efficiency} = \frac{1}{\pi} \int_0^{2\pi} \int_0^{R+\rho_{\max}} \frac{h^{n+1}\, r'\, dr'\, d\gamma}{\left[r'^2 + 2r'D\cos\gamma + h^2 + D^2\right]^{\frac{n+3}{2}}}, \qquad (11)$$

where n is the exponent of the cosine as in Eq. (4), $\rho_{\max}$ is the maximum radial extent of the planet, and all other variables are as shown in Fig. 94.2. The efficiency can then be calculated for a range of source offsets for a given plantary geometry. The results of these efficiency calculations are shown for the counter-rotating geometry in Fig. 94.3.

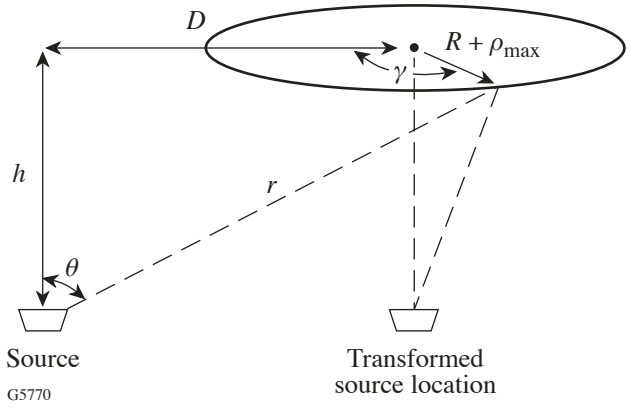

Figure 94.2
Deposition efficiency is calculated by transforming the source location to a position on-axis with the rotation and integrating over the maximum area described by the planetary motion, a disk with radius $R + \rho_{\max}$.

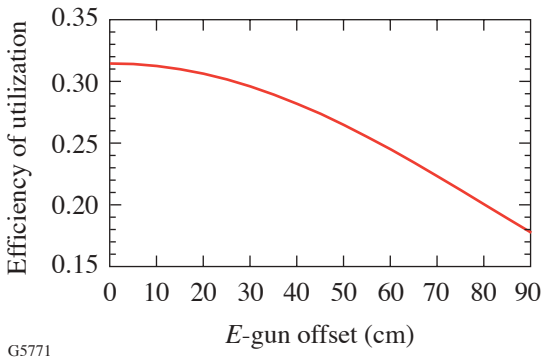

Figure 94.3
Efficiency of material utilization as a function of the offset of the source from the center of the coating chamber. An offset of 0 is for source location (0, 0, z_s) in Fig. 94.1, with increasing offsets representing the movement of the source along the x axis. While there is a significant reduction in the efficiency of the material being evaporated, the reduction in the size of secondary masking may offset this loss.

The efficiency of material utilization may be somewhat misleading since this considers only whether the material is available for use, not where the material would condense on the substrate and its impact on the film uniformity. To make an informed analysis of the actual material utilization, one must take into account any masking required to achieve a uniform deposition.

Measurement of Film Uniformity

Many different coating designs are required for the NIF, but all use the same evaporant materials with layer deposition times greater than 4 min, with a planetary revolution period of approximately 6 s. Therefore, the uniformity of the deposition process will be qualified for NIF specifications, assuming the deposition of similar layers will not deviate substantially from the measured uniformity.

To improve film uniformity, it is first necessary to accurately measure the achieved uniformity. A large-aperture scanning laser photometer installed at LLE is capable of mapping transmission and reflection performance of a NIF-sized (525 × 807-mm) optic (Fig. 94.4). Since this instrument measures photometric performance at a single wavelength, it is necessary to develop a correlation between transmission of the coating and film uniformity. Furthermore, to increase the accuracy of the measurement, the transmitted light should be highly sensitive to thickness nonuniformities, with a maximum range of transmitted light.

G5772

Figure 94.4
Scanning laser photometer at LLE. This system is capable of simultaneously measuring % T and % R over a 525 × 807-mm aperture, from 8° to 60°, at wavelengths of 1053, 527, and 351 nm. Results are presented as a 2-D intensity map of the surface, digitized to pixels of 1 to 5 mm.

A modified quarter-wave reflector was designed such that the edge of the reflectance band is approximately linear with respect to wavelength (Fig. 94.5). Since the photometer operates at 1053 nm, a slope of 1% T per nanometer correlates to a relationship of 1% T per 0.1% thickness nonuniformity. When a large coated substrate is then mapped on the photometer, changes in transmittance will indicate the shifting of the spectral performance of the coating to the left or right in Fig. 94.5, for higher or lower values of % T respectively. If the slope of the reflectance band is verified on a spectrophotometer, the precise correlation of transmittance to thickness change can then be established for a given coating deposition since the percent wavelength shift of the coating performance will be equal to the percent change in coating thickness. This is typically adequate for initial uniformity efforts, although further reduction of nonuniformity may require coatings that have a more steeply sloped transmission profile and therefore are more sensitive to slight film nonuniformities.

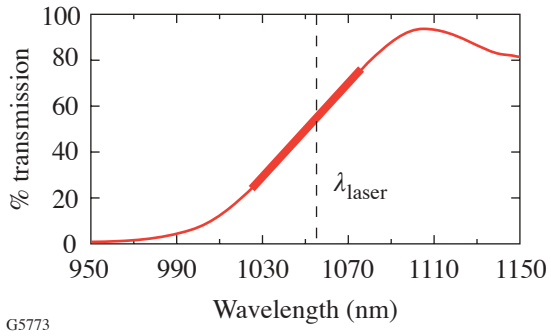

G5773

Figure 94.5
Modified quarter-wave reflector with linear transmission with respect to wavelength over the range $\lambda_0 \pm 2\%$. Provided the coating is deposited properly and all nonuniformities are less than 4% peak-to-valley, the resulting photometer transmittance map will directly correlate to film-thickness uniformity.

Planetary Gearing

The essence of a planetary rotation system in a vacuum coating chamber is that the substrate holder, or planet, will undergo planetary motion by rotating about its center axis while revolving about the center axis of the coating chamber. The planet will continue to move through the vapor plume of the evaporation source in this manner, allowing the deposited film thickness to become more uniform by averaging the different regions of the plume incident on each portion of the planet. The most basic system is a two-gear system, as depicted in Fig. 94.1. The center "solar gear" remains stationary, and the outer "planet gear" rotates while revolving about the center of the system.

Many thin-film-uniformity calculations assume that a sufficient number of revolutions take place during a layer deposition that the calculations of thickness uniformity can be reduced to an integration over the planet radius,[7] with the corresponding assumption that the film is "perfectly uniform" for constant planet radius. This would mean that all film nonuniformity would be only in the radial direction in a polar coordinate

system. In reality, the relative sizes of planetary and solar gears are critical to achieving high degrees of thickness uniformity. If the solar gear has a number of teeth equal to "N_s" and the planet gear has a number of teeth equal to "N_p," then the gear ratio is given by

$$\text{Gear ratio} = \frac{N_s}{N_p}. \tag{12}$$

This gear ratio determines the number of rotations the planet will make for each revolution of the planetary fixture, causing each point on the planet to trace out a cycloid during each revolution based on Eqs. (8) and (9). Beginning with the simplest case of a gear ratio equal to 1, it is apparent that successive revolutions of the planetary will trace identical circles since each revolution of the planet also corresponds to a single rotation; this eliminates the benefit of planetary motion since a given point will travel an identical path through the vapor plume, failing to average differing plume conditions [Fig. 94.6(a)]. Typically, the gear ratio is not equal to 1, but instead, due to planetary geometry, $N_s > N_p$. If the gear ratio is an integer greater than 1, identical cycloids will be traced out for each successive revolution, severely limiting the degree of random motion [Figs. 94.6(b)–94.6(f)]. It has been known for some time that the gear ratio must be non-integral,[5] such that the cycloid traced out is no longer a closed figure and therefore will not be repeated with each successive revolution.

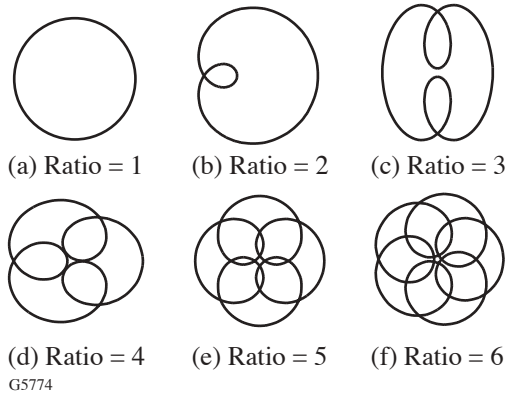

Figure 94.6
Cycloids traced out by an off-center point in a planetary rotation after one revolution with different integral gear ratios. Note that all figures are closed, requiring that the point will trace out an identical path for all successive revolutions.

The limitations on this next level of randomization can also be expanded by examining how quickly a given cycloid will be repeated. If the gear ratio is non-integral, this indicates that the planet will not reach its starting angular orientation at the conclusion of one revolution of the planetary. Therefore, the cycloid traced out by the previous revolution cannot be repeated in the next revolution since the revolution did not trace out a closed figure. Each successive revolution will provide an opportunity for the planet orientation to achieve its starting position and therefore repeat its path through the vapor plume. The path will not repeat until

$$m\left(\frac{N_s}{N_p}\right) = \text{an integer} \qquad m = 1, 2, 3, \ldots, \tag{13}$$

where m is the number of revolutions of the planetary, since this represents an integral number of rotations of the planet and therefore closes the figure traced by the cycloid. Since N_s and N_p are both integers, the maximum possible number of revolutions before the system repeats is $m = N_p$. In the event that N_p and N_s have common factors, the ratio simplifies and repetition of the path through the vapor plume will occur at

$$m = \frac{N_p}{g}, \tag{14}$$

where g is the greatest common factor of N_p and N_s.

The previous condition requiring no common factors is sufficient to establish unique paths through the vapor plume, but again it is insufficient to minimize film nonuniformities in practice. Since the maximum number of paths is equal to N_p, every path will be used exactly once only for those layers of the appropriate thickness such that the deposition time is equal to N_p multiplied by the period of revolution of the planetary, or an integer multiple thereof. In practice, this condition is rarely if ever met due to variations in deposition rate, design layer thickness, and material being deposited. In this event, paths that are similar to one another are sufficient to cause greater degrees of nonuniformity, and the fewer the number of revolutions of the planetary, the greater the observed impact on uniformity. If the angular orientation of the planet is tracked and plotted at a fixed point in the revolution, such as the center of the door of the chamber, it can be shown how the paths relate to one another. As shown in Fig. 94.7 for the given values of $N_s = 237$ and $N_p = 71$, the planet starts with the arrow denoting its orientation at 0°. After one revolution, the planet has undergone 3 full rotations plus an additional partial rotation, resulting in a change in orientation of 121.69°. After the second revolution, the planet will again have undergone 3 complete rotations plus an additional 121.69°, resulting in an orientation

of 243.38°. The third revolution will nearly return the planet to its starting orientation, differing only by 5.1°. This will repeat for successive revolutions such that, for the given configuration, every 3 revolutions the planet will return to almost the same orientation. The graphs in Fig. 94.8, I(a)–I(c), plot the angular orientation of a planet as a function of the number of revolutions the planetary has undergone for different gear configurations. Tracking the planet in such a manner, it is possible to see that the planet assumes approximately the same angular orientation every 3 revolutions for configuration (a), every 4 revolutions for configuration (b), and every 13 revolutions for configuration (c). The graphs labeled II(a)–II(c) show the path traced by a point on the planet through 30 revolutions of the planetary rotation. Especially when depositing thin layers, this near-repetition is evident in the symmetry observed in the measured film uniformity. The surface plots in Row III of Fig. 94.8 provide experimental evidence of rotational nonuniformity due to inappropriate gearing, and 3-, 4-, and 13-way symmetries are apparent in the measured film thickness. As higher degrees of symmetry are reached, it becomes much more difficult to resolve these effects and the uniformity is significantly improved.

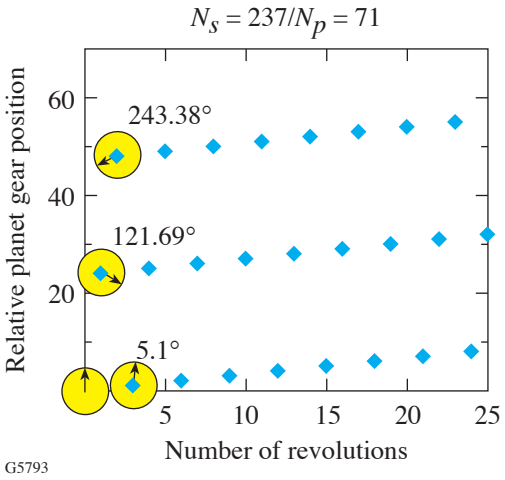

Figure 94.7
Relative planar orientations versus revolutions of the planetary rotation. Every 3 revolutions, the planet assumes almost the same angular orientation, differing only by 5.1°.

Uniformity Masking

Once a stable deposition system has been configured, with optimized planetary gearing, the residual thickness nonuniformities can be removed through the use of masking. Most planetary rotation geometries will result in the center of the planet having a thicker film deposited than the periphery; therefore the mask will be required to obscure a greater percentage of the center each revolution. There are multiple methods of masking the vapor plume, including large masks rotating in the opposite direction as that of the planetary,

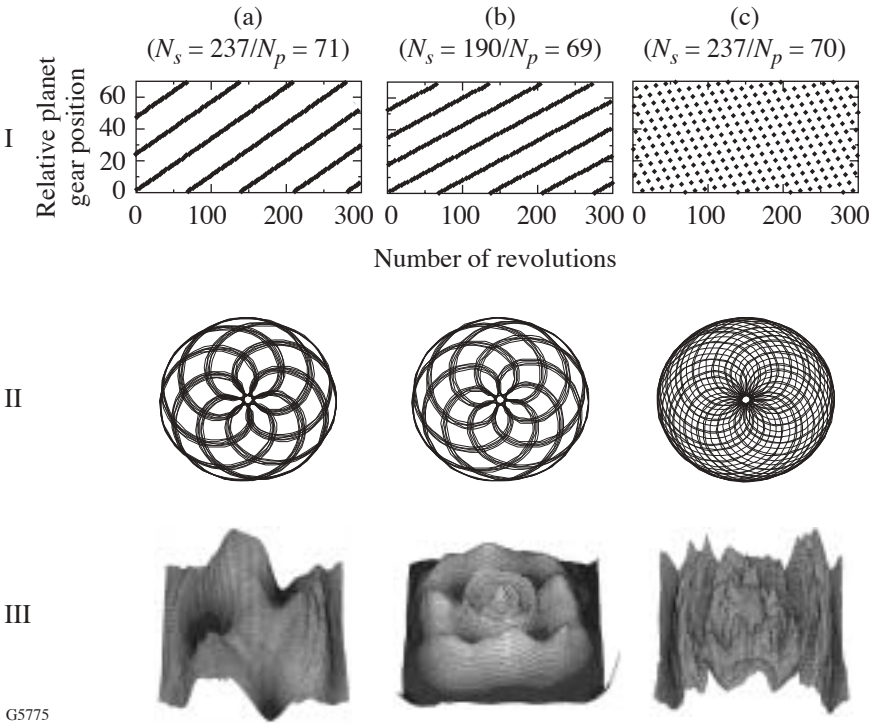

Figure 94.8
Comparison of the effects of different planetary gear ratios. The graphs in Row I track the angular orientation of a planet each time it passes a fixed point in the chamber, such as the center of the door, as a function of the number of revolutions of the planetary. Since a geared system is being analyzed, the possible angles correspond to a specific gear tooth number. Row II depicts the path of an off-center planetary point through 30 revolutions of the planetary. Row III depicts the measured film uniformity pattern on the mapping laser photometer. Gearing configuration (c) provides a greater degree of randomization through the vapor plume, yielding significant improvements in film uniformity.

individual masks for each planet that are rotated with the planetary, and fixed-position uniformity masks. The fixed-position masking is the lowest-maintenance, highest-mechanical-reliability system so is therefore preferred, provided it is capable of meeting the nonuniformity requirements of the coatings. A critical aspect of this masking system is the proper mounting of the masks in the coating chamber; the masks must be placed precisely in the position defined by the model, using a mounting structure that is stable and repeatable and that takes thermal expansion into account if the effect on mask placement warrants. Small changes in the mask shape can have a significant impact on the film uniformity, and care must be taken to avoid changes due to poor mounting.

A model was created to sum thickness contributions over the aperture of a planet as it undergoes planetary rotation, according to Eqs. (4)–(9) above. The model accounts for the motion of the planet due to the gearing and relies on plume shape fitting by varying n in Eq. (4). Masks are projected onto the plane in which the planet surface moves, providing a binary multiplier to the thickness contribution at that point. Mask shapes are determined by evaluating the film distribution and altering the mask width as needed at the appropriate radii in the planetary.

We have found that the optimal mask shapes for a standard planetary rotation system have a very smooth, continuous shape, providing minimal difficulty in manufacture, installation, or usage; this also results in an absence of high-frequency, high-gradient thickness changes. The primary focus of this work, however, was to improve uniformity over a large-aperture optic for the NIF laser system suspended in a counter-rotating planetary, as shown in Fig. 94.9. The fact that the optic crosses the center of the coating chamber, and may experience masking effects intended for a different radius on the optic, poses significant challenges in creating a suitable mask shape. In spite of this, the basic model is identical to that used for a standard planetary system, although the aperture over which the coating must be uniform is significantly larger.

The source placement and characteristics have a significant impact on the uniformity of the film thickness prior to the use of masking. As shown in Fig. 94.10, changes in the source placement can vary the degree of nonuniformity over a range of 17.6% to 2.4% for source positions of 0 to 90-cm offset from the center of the planetary, respectively, for a 90-cm-aperture optic in the counter-rotating planetary. Exact performance will be highly dependent upon the geometry of the particular planetary rotation. A source offset of 90 cm was the maximum considered since this would correspond to placing the source in the corner of the 72-in. coating chamber. Some of the standard arguments against placing the source a significant distance off-center in a planetary include the following:

1. The material utilization of the source will be significantly decreased.
2. The chamber walls will influence the vapor plume, causing undesirable effects.
3. The higher angles of the vapor plume, which are more erratic, will be used, resulting in reduced consistency of the uniformity.


G5789

Figure 94.9
Mask configuration implemented in a 72-in. coating chamber for a counter-rotating planetary. Multi-point quartz crystal monitoring is installed in the mask mounts, providing six thickness/rate measurements.

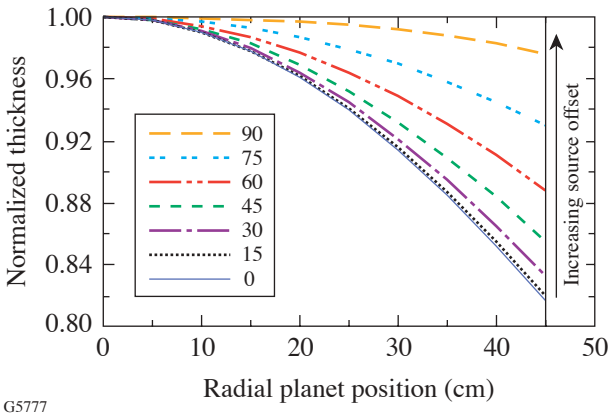

G5777

Figure 94.10
Theoretical uniformity of film deposition over the radius of the planet versus offset of the source position from the center of the coating chamber, for $z_p - z_s$ = 1200 mm, R = 391 mm, and n = 1.6. By minimizing the nonuniformity of the deposited film, the degree of secondary masking may also be minimized.

While the material utilization is decreased, as shown in Fig. 94.3, the decrease in the amount of masking required to produce a uniform deposition results in an equivalent, or even improved, material utilization once the masked configuration is considered. Wall effects are possible, but it was decided to proceed with the configuration change and experimentally determine if this effect is significant. As demonstrated in the uniformity results shown below, as well as by laser-damage testing, the influence of the wall proximity was not an issue. As for the possibility of increased sensitivity, thickness uniformity was modeled for differing plume shapes once a masked configuration was developed for different radial offsets of the source. The model indicates that the uniformity is actually more stable for the source positions that are farther off-axis in the planetary, as shown in Fig. 94.11.

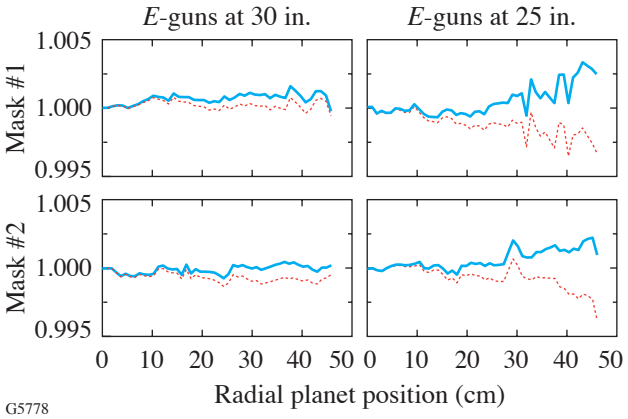

Figure 94.11
Theoretical influence of source offset on the sensitivity of film uniformity to changes in the vapor plume distribution. Source distribution modeled as $\cos^{1.6}\theta$, with n varying ±0.2. Two significantly different mask designs are modeled, each with two source offsets, showing that the greater source offset is actually less sensitive to variations in the vapor plume.

Results

Uniformity masks have been produced for a number of different chamber configurations, and the experimental results have been mapped on the scanning laser photometer. First, a value of n in Eq. (4) is assumed in the model, appropriate masking is designed to correct the thickness nonuniformities, and a deposition is performed on a large-aperture substrate. The transmittance is then mapped on the laser photometer, the correlation of transmittance to thickness is determined based on a spectral measurement at one point in the planet, and the resulting nonuniformity is calculated. In order to improve upon this result, the variable n must now be adjusted to best-fit the model to the experimentally determined nonuniformity. All other quantities, such as the source and substrate locations, mask shapes and locations, and planetary gearing, are physically measured quantities known to a high degree of precision. Once the model accurately predicts the results achieved, the model may be used to redesign the masks to correct the remaining nonuniformities, repeating the process until the degree of nonuniformity is acceptable. Typically, deviations in the best-fit process were found to be less than 0.1% except at the extremes of the substrates, where variations could reach 0.15%. Figure 94.12 illustrates the nonuniformity achieved for a 24-layer coating with layer thicknesses of approximately $\lambda/4$ at 900 nm in a 72-in. counter-rotating planetary. Edge roll-off is evident in the data due to shadowing of the coating tooling along the edges of the substrate. Typical model performance has yielded nonuniformity of less than 1% over the aperture of interest in one to two masking iterations. The primary goal—to achieve good uniformity over a full NIF aperture—was completed in two mask iterations, with a final film nonuniformity of 0.45% peak-to-valley, after removal of roll-off. Correction of tilt in the planet would allow this to be further reduced to 0.30%; while this is a 33% reduction in the nonuniformity, it is relatively insignificant compared to optic specifications, and the necessary modifications cannot be justified.

Conclusions

Highly uniform thin films for large-aperture, high-precision optical coatings have been deposited with stationary masking and planetary rotation utilizing the two-gear, counter-rotating configuration. Impacts on nonuniformity due to planetary gearing have been measured, the causes investigated, and appropriate corrections applied to minimize rotational nonuniformities in film thickness. The model developed has been shown to be effective in designing suitable masks to correct thickness nonuniformities. While further improvements are certainly possible through the use of rotating masks, friction-drive planetary rotation, or three-gear configurations, the simplicity and reliability of the current system make its continued use highly desirable. Furthermore, the results achieved significantly exceed the uniformity requirements for NIF laser coatings, despite the complexities of the counter-rotating planetary.

Further improvements to the uniformity masking model are planned in two primary areas: (1) a better description of the vapor plume to more accurately fit the measured results at higher angles and (2) automated optimization of the mask shape. The masking concept can also be further improved by

making the masks asymmetric, to account for differences in the shapes of the vapor plumes of the individual sources. The described configuration has been shown to work well for the deposition of layers >4-min duration, with a planetary period of approximately 6 s. It is expected that layers with significantly shorter deposition times will require higher planetary speeds or will necessitate the use of additional enhancements to the planetary/masking system, such as the use of rotating masks.

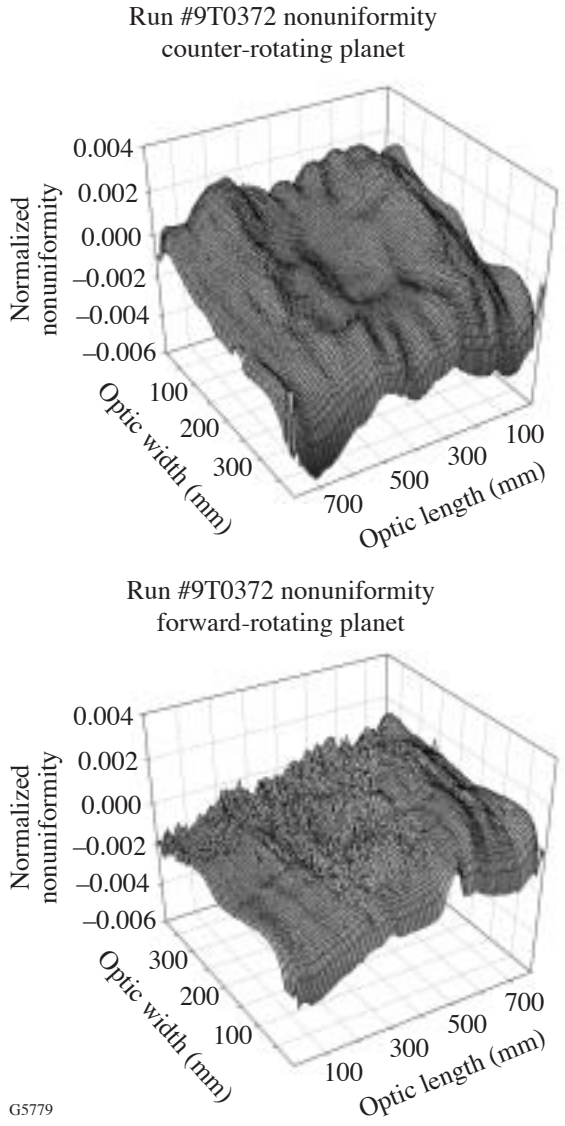

Figure 94.12
Film nonuniformity in both the counter-rotating and forward-rotating planets for a masked configuration with electron-beam sources at 76-cm offset from chamber center. Roll-off is evident along the length of the coating due to shadowing effects of the coating tooling. Discounting this effect, which may be eliminated by modification of the coating tooling, both uniformity maps exhibit 0.45% nonuniformity peak-to-valley. Furthermore, if the tilt evident in both surface plots is subtracted, since this is a result of the optic rotating out-of-plane, nonuniformity is reduced to 0.30%.

ACKNOWLEDGMENT

This work was supported by the U. S. Department of Energy Office of Inertial Confinement Fusion under Cooperative Agreement No. DE-FC03-92SF19460, the University of Rochester, and Lawrence Livermore National Laboratories under subcontract B399901. The support of DOE does not constitute an endorsement by DOE of the views expressed in this article.

REFERENCES

1. I. C. Stevenson and G. Sadkhin, in *Proceedings of the 44th Annual Technical Conference of the Society of Vacuum Coaters* (Society of Vacuum Coaters, Albuquerque, NM, 2001), pp. 306–313.
2. D. J. Smith *et al.*, in *Proceedings of the 41st Annual Technical Conference of the Society of Vacuum Coaters* (Society of Vacuum Coaters, Albuquerque, NM, 1998), pp. 193–196.
3. B. Andre, L. Poupinet, and G. Ravel, J. Vac. Sci. Technol. A **18**, 2372 (2000).
4. R. Chow *et al.*, Appl. Opt. **32**, 5567 (1993).
5. B. S. Ramprasad and T. S. Radha, Thin Solid Films **15**, 55 (1973).
6. K. H. Behrndt, in *Transactions of the Tenth National Vacuum Symposium of the American Vacuum Society*, edited by G. H. Bancroft (The Macmillan Company, New York, 1963), pp. 379–384.
7. A. G. Zhiglinskiy and E. S. Putilin, Opt.-Mekh. Prom. **38**, 46 (1971).
8. H. A. Macleod, *Thin-Film Optical Filters*, 3rd ed. (IOP Publishing, Bristol, England, 2001), pp. 488–497.
9. A. Musset and I. C. Stevenson, in *Proceedings of the 31st Annual Technical Conference of the Society of Vacuum Coaters* (Society of Vacuum Coaters, Albuquerque, NM, 1988), pp. 203–209.